

Developing Vasculature and Stroma in Engineered Human Myocardium

Kareen L. Kreutziger, Ph.D.,^{1,2} Veronica Muskheli, M.S.,^{1,2} Pamela Johnson, Ph.D.,³ Kathleen Braun, B.S.,³
Thomas N. Wight, Ph.D.,^{2,3} and Charles E. Murry, M.D., Ph.D.^{1,2,4,5}

We recently developed a scaffold-free patch of human myocardium with human embryonic stem cell-derived cardiomyocytes and showed that stromal and endothelial cells form vascular networks *in vitro* and improve cardiomyocyte engraftment. Here, we hypothesize that stromal cells regulate the angiogenic phenotype by modulating the extracellular matrix (ECM). Human marrow stromal cells (hMSCs) support the greatest degree of endothelial cell organization, at 1.3- to 2.4-fold higher than other stromal cells tested. Stromal cells produce abundant ECM components in patches, including fibrillar collagen, hyaluronan, and versican. We identified two clonal hMSC lines that supported endothelial networks poorly and robustly. Interestingly, the pro-angiogenic hMSCs express high levels of versican, a chondroitin sulfate proteoglycan that modulates angiogenesis and wound healing, whereas poorly angiogenic hMSCs produce little versican. When transplanted onto uninjured athymic rat hearts, patches with proangiogenic hMSCs develop ~50-fold more human vessels and form anastomoses with the host circulation, resulting in chimeric vessels containing erythrocytes. Thus, stromal cells play a key role in supporting vascularization of engineered human myocardium. Different stromal cell types vary widely in their proangiogenic ability, likely due in part to differences in ECM synthesis. Comparison of these cells defines an *in vitro* predictive platform for studying vascular development.

Introduction

REPLACEMENT OF CARDIOMYOCYTES after myocardial infarction has become an important therapeutic objective because of the heart's inability to regenerate. These cell-based cardiac therapies have evolved from initial successes using direct cell injection into the infarct¹⁻³ and now include many tissue engineering approaches, including scaffold-based⁴⁻⁶ and scaffold-free engineered constructs.^{7,8} Recently, we and others have begun incorporating vascular cells into these constructs to promote the survival of engrafted cardiomyocytes.⁹⁻¹² We showed that human cardiomyocyte graft size increases by >10-fold with addition of endothelial cells and fibroblasts to human embryonic stem cell (hESC)-derived cardiomyocytes in scaffold-free cardiac tissue patches.¹¹ Therefore, the importance of providing a vasculature to nourish transplanted cardiomyocytes suggests a need for further development of vascular structures in three-dimensional engineered tissue constructs.

The engineering of vascular structures *in vitro* requires both an endothelial cell source and a support cell, such as dermal fibroblasts, marrow stromal cells (MSCs), or peri-

cytes.¹³ Multi-cell cultures have been used in tissue engineering by mixing purified cells in culture^{9-11,14} or by obtaining heterogeneous primary biopsy cultures.⁴ Vessel structures have been created in constructs by self-assembly of endothelial cells,^{11,14} bioprinting,¹⁵⁻¹⁷ or implantation on the omentum,¹⁸ and the inclusion of stromal cells increases endothelial cell survival and proliferation.^{11,19} In addition to promoting angiogenesis via direct contact and paracrine signaling (reviewed in Ref.²⁰), stromal cells produce extracellular matrix (ECM). In native tissue the ECM plays an important role in regulating endothelial cell behavior in vascular homeostasis, angiogenesis, and disease (reviewed in Refs.²¹⁻²⁴). We hypothesized that the stromal cell population predominantly creates the ECM environment of our scaffold-free engineered cardiac tissue patches, and that this ECM promotes the observed proangiogenic phenotype of endothelial cells.

In the current study, we demonstrate that different stromal cell types support *in vitro* endothelial cell network formation with varying success, and that human mesenchymal stem cells are the most capable of the cells we tested. We show that, whereas cardiomyocyte preparations can produce

¹Center for Cardiovascular Biology, Institute for Stem Cell and Regenerative Medicine, University of Washington, Seattle, Washington.

²Department of Pathology, University of Washington, Seattle, Washington.

³Benaroya Research Institute at Virginia Mason, Hope Heart Program, Seattle, Washington.

Departments of ⁴Bioengineering and ⁵Medicine/Cardiology, University of Washington, Seattle, Washington.

ECM in the absence of stromal cells, the matrix in tri-cell patches is predominantly produced by the stromal cells. Using clonal human MSCs (hMSCs) with different gene expression levels of ECM components,²⁵ we show that the ability to promote vascular networks correlates with production of the proteoglycan versican. Finally, we demonstrate that upon implantation in uninjured athymic rat hearts, tissue-engineered cardiac patches that had robust human endothelial cell networks *in vitro* form human–rat chimeric vessels *in vivo*, whereas patches made with the poorly angiogenic stromal cells do not. These data suggest that selection of stromal cells is important for development of the ECM and prevascular endothelial cell networks in engineered human cardiac tissue patches, which can be used as an *in vitro* platform for studying endothelial cell network formation.

Materials and Methods

Culture of hESCs and derivation of cardiomyocytes

Undifferentiated H7 hESCs were maintained as previously described.⁷ Cardiomyocytes were derived from hESCs as previously described,¹ which yielded 22%–35% beta-myosin heavy chain (β MHC)-positive cardiomyocytes. Briefly, undifferentiated hESCs were plated at 100,000 cells/cm² on Matrigel-coated plates (Growth Factor Reduced Matrigel; BD Biosciences) and when they formed a super-confluent, tightly packed monolayer, directed differentiation was initiated with addition of 50 ng/mL activin A (R&D Systems) for 24 h, followed by 10 ng/mL BMP4 (R&D Systems) for 4 days in the RPMI medium (Gibco) with 1 \times B27 supplement (Gibco). The medium was replaced every 2 days until beating cardiomyocytes were observed, which were harvested for use in tissue-engineered patches.

Creating scaffold-free vascularized human cardiac tissue patches

Scaffold-free human cardiac tissue patches were made in ultra-low attachment six-well plates (Corning) on a rotating orbital shaker as previously described.⁷ Disk-shaped patches of ~400 μ m thickness formed within 2 days by hydrodynamic forces and cell–cell adhesion. Culture of human umbilical vein endothelial cells (HUVECs; Lonza) was as previously described.¹¹ Culture of primary hMSCs (Lonza) was according to manufacturer's recommendations using the MSCGM medium (Lonza). Human MSC clones HS-27a and HS-5²⁶ were cultured on uncoated plates in Dulbecco's modified Eagle's medium (Gibco) with 5% fetal bovine serum (HyClone) and 2 mM L-glutamine. HESC-derived cardiomyocytes were enzymatically dispersed with TrypLE (Gibco) and gently triturated⁷; HUVECs were enzymatically dispersed with 0.025% Trypsin in versene (0.5 mM EDTA and 1.1 mM D-glucose [Gibco] in phosphate-buffered saline [PBS]); primary hMSCs and clonal hMSCs were enzymatically dispersed with 0.05% Trypsin in versene. Cells were mixed in ratios of 1:1 for cardiac:HUVEC patches, 1:1:0.5 for cardiac:HUVEC:stromal cell patches, or 1:0.5 for HUVEC:stromal cell patches with 1–2 \times 10⁶ cardiomyocytes (and/or HUVECs) per patch for *in vitro* studies or 5 \times 10⁶ cardiomyocytes for implants. Tri-cell patches were fed with a human embryoid body medium (huEB; 80% KO-Dulbecco's

modified Eagle's medium [Gibco], 20% fetal bovine serum [HyClone], 1 mM L-glutamine, 0.1 mM β -mercaptoethanol, and 1% nonessential amino acids) and bi-cell patches were fed with 50/50 v/v huEB and endothelial growth medium 2 (Lonza). For conditioned medium experiments, huEB/endothelial growth medium 2 was added at 10 mL per 148 cm² (half of normal feeding volume) to plates of HS-5 or HS-27a hMSCs that were 70%–100% confluent for 24 h.

Immunohistochemistry and microscopy

Patches were rinsed in PBS, fixed in methanol with 10% acetic acid (v/v) or 4% paraformaldehyde, and routinely processed for paraffin embedding. Sections (5 μ m) were cut parallel to the major patch plane or from hearts receiving patch implants and labeled with various antibodies, biotinylated proteins, or histochemical stains to identify cell populations and ECM components. Immunohistochemistry and immunofluorescence are as previously published¹¹ for β MHC (clone A4.951, 1:10 dilution of hybridoma supernatant; American Type Culture Collection) to identify human cardiomyocytes; human CD31 (hCD31; monoclonal mouse anti-human CD31, 1:20 dilution; Dako) to identify HUVECs; TER-119 (PE-conjugated antibody, 1:400 dilution; BD Pharmingen) to identify erythrocytes; and picosirius red to identify fibrillar collagen. In some patches, rabbit CD31 (polyclonal rabbit anti-CD31, 1:800; Novus) is used to identify HUVECs with the same protocol as hCD31 except with biotinylated goat anti-rabbit IgG (1:500; Jackson Labs) as secondary antibody. Observation was with 1,3-diaminobenzidine (brown staining; Vector Laboratories) and counterstained with hematoxylin for light microscopy or by Alexa 488- or Alexa 596-conjugated secondary antibody for fluorescence. For identifying rat versus human endothelium in heart sections, sections were blocked with 1.5% normal goat serum in PBS and rat endothelial cell antigen (RECA; mouse anti-RECA-1, 1:10 dilution; Novus) primary antibody was used with sheep anti-mouse HRP IgG secondary antibody (1:100; GE Healthcare) and Tyramide Signal Amplification Kit with Alexa 488 (Invitrogen). This was followed by mouse anti-human CD31 (1:10; Dako) primary antibody and goat anti-mouse IgG Alexa 594 (1:500; Invitrogen) secondary antibody. For immunofluorescence, sections were counterstained with 4',6-diamidino-2-phenylindole and coverslipped with VectaShield (Vector Laboratories). Immunohistochemistry for hyaluronan (HA) and mouse versican is as previously described²⁷ and details are below for human versican staining. Biotinylated HA binding protein (2.5 μ g/mL; Sigma) identifies HA; a rabbit anti-mouse versican antibody against β GAG (7 μ g/mL; AB1003; Millipore) identifies mouse versican; and a monoclonal mouse anti-human versican antibody (2B1; 0.25 μ g/mL; Seikagaku) identifies human versican. The protocol and secondary antibodies are as previously published²⁷ with the following modifications for human versican: initial blocking was with 10% normal goat serum and 1% BSA in PBS (1 h, 37°C) and secondary antibody was biotinylated goat anti-mouse IgG (1:300; Vector Laboratories). Observation was with the chromagen Vector Red or Nova Red (pinkish-red staining; Vector Laboratories) and sections were counterstained with hematoxylin. Bright-field images were obtained on an Olympus BX41 microscope with a Scion camera (Model CFW-1312C; Scion Corporation), and immunofluorescent images

were obtained with a confocal microscope (Zeiss LSM510 META).

Quantification of vessel-like structures

In sections stained for CD31, vessel-like structures were identified as lumen-like or cord-like structures. Lumen-like structures had continuous endothelial cells (≥ 1 cell) in a circular morphology and cord-like structures had elongated endothelial cells with end-to-end contact (≥ 2 cells). About 4–10 randomly dispersed fields were counted per patch (average 8.5 ± 0.4 fields per patch) by a trained technician who was blinded to treatment group ($n = 3$ patches per group). Total vessel-like structures are reported as the sum of lumen-like and cord-like structures and normalized by area. Measurements of lumen diameter on hCD31-stained sections were made across the shortest distance, so that values represent a lower limit to vessel diameters.

RNA isolation and quantitative reverse transcriptase-polymerase chain reaction

All reagents were supplied by Applied Biosystems. cDNA was prepared from 500 ng total RNA, reverse transcribed in a 30 μ L reaction mix with random primers using the High-Capacity cDNA Reverse Transcription Kit according to manufacturer's instructions. Relative quantification of versican gene expression of isoforms V0, V1, V2, and V3 was performed using TaqMan Gene Expression Assays Hs01007944_m1, Hs01007937_m1, Hs01007943_m1, and Hs01007941_m1, respectively. Expression was normalized to eukaryotic 18S rRNA Endogenous Control part no.4333760. Briefly, 17 ng cDNA was amplified in 1XTaqMan Fast Universal PCR Mix with 250 nM TaqMan probe in a 20 μ L reaction using the Fast program for 50 cycles on an ABI7900HT thermocycler. All samples were done in duplicate, and data were analyzed using the Comparative CT Method with software from Applied Biosystems. Estimated copy numbers from CT values were generated from a standard curve created by using a selected reference cDNA template and TaqMan probe.²⁸

Implantation in uninjured nude rat hearts

All animal procedures were conducted in accordance with U.S. National Institutes of Health Policy on Humane Care and Use of Laboratory Animals and approved by the University of Washington (UW) Animal Care Committee. Rats were housed in the Department of Comparative Medicine and cared for in accordance with UW Institutional Animal Care and Use Committee procedures. Implantation of patches on uninjured hearts of athymic Sprague Dawley rats is as previously described.¹¹ Briefly, rats were anesthetized with isoflurane, intubated, and mechanically ventilated. A thoracotomy exposed the heart and the pericardium was opened. To enhance survival, patches were treated with heat shock at 42°C for 30 min 1 day before implantation and prepared in a pro-survival cocktail as previously described.¹ One patch was implanted per heart with 3–5 stitches using 8–0 suture ($n = 2$ C:H:HS-5 patches; $n = 4$ C:H:HS-27a patches; $n = 2$ C:H:primary hMSC patches). The chest was closed aseptically and animal recovery was monitored. To prevent patch cell death via mitochondrial pathways, animals received cyclosporine A (0.75 mg/day; Wako Pure

Chemicals) subcutaneously for 1 week beginning 1 day before implantation. Animals were sacrificed 1 week after patch implantation and all patches were found. Hearts were sectioned through the short axis in the center of the patch so that the largest area through the depth of the patch could be analyzed for cellular and vascular content. Samples were fixed in Methyl Carnoy's fixative, processed, and paraffin-embedded for sectioning and histology. One or two sections per heart (patch area of 2.4 ± 0.1 mm²; average \pm SEM) were analyzed for vessel-like structure count and diameter.

Statistical analysis

Statistical significance ($p < 0.05$) was determined using a two-tailed Student's *t*-test assuming unequal variance (Fig. 1) or a one-tailed Student's *t*-test assuming equal variance (Fig. 3). Error bars represent SEM for all measurements except where SD is reported for lumen diameter.

Results

Human stromal cells improve endothelial cell networks

In developing a clinically relevant human cardiac tissue patch, our first goal was to find a source of human stromal cells to support endothelial cell networks. Using our tri-cell patch culture system, we tested hESC-derived cardiomyocytes and HUVECs with either neonatal human dermal fibroblasts (NHDFs) or primary human MSCs (hMSCs; Fig. 1). At 8 days of culture, all patches contained numerous cardiomyocytes expressing β MHC (Fig. 1A, inset). When stained for human endothelium using a human-specific CD31 antibody, cardiac-only and cardiac:HUVEC patches exhibited few vessel-like structures (Fig. 1A, B). As previously observed,¹¹ addition of mouse embryonic fibroblasts (MEFs) supported the development of *in vitro* endothelial cell networks, characterized by the formation of lumen-like and cord-like vessel structures (Fig. 1C). Use of NHDFs or hMSCs in the tri-cell patches also supported the development of these vessel-like structures (Fig. 1D, E) and, interestingly, both human stromal cell types supported more vessel-like structures than patches derived using MEFs (Fig. 1F). Therefore, we created a fully human-derived cardiac tissue patch with improved vessel structure development *in vitro*.

ECM deposition by stromal cells

Because cell–matrix interactions can have profound effects on cell physiology and angiogenesis,²¹ we explored the nature of the ECM produced by cells in the patch. Cardiac patches stained with picosirius red showed increased fibrillar collagen content with addition of stromal cells (Fig. 2A–C), as we previously demonstrated.¹¹ HA is the only unsulfated glycosaminoglycan of the ECM in mammals and plays important roles in endothelial cell behavior (reviewed in Ref.²⁹). We found that HA was widespread and abundant in cardiac-only, cardiac:HUVEC, and cardiac:HUVEC:MEF patches, with no appreciable difference among groups (Fig. 2D–F). Versican is a large HA-binding chondroitin sulfate proteoglycan that is abundant in vessel walls, regulates cell adhesion, proliferation, and migration,³⁰ and plays a role in angiogenesis and vascular response to injury.³¹ Interestingly, whereas total versican content did not vary among patches with different cell compositions, use of two

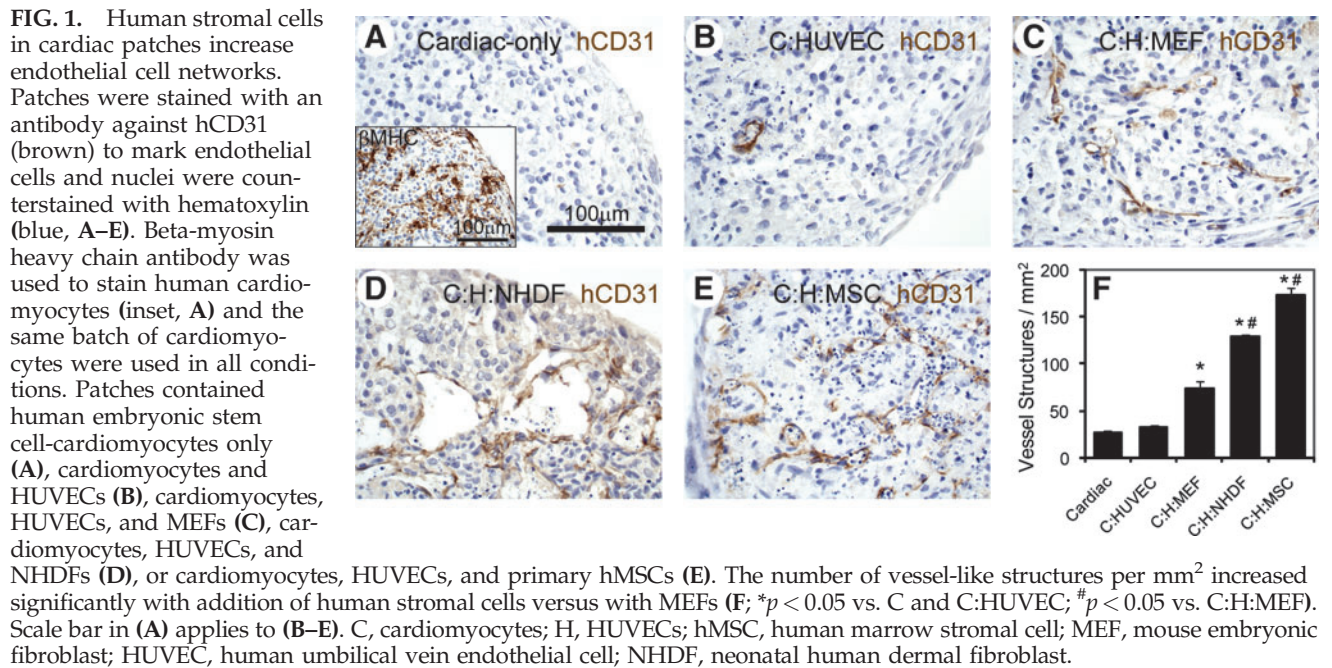
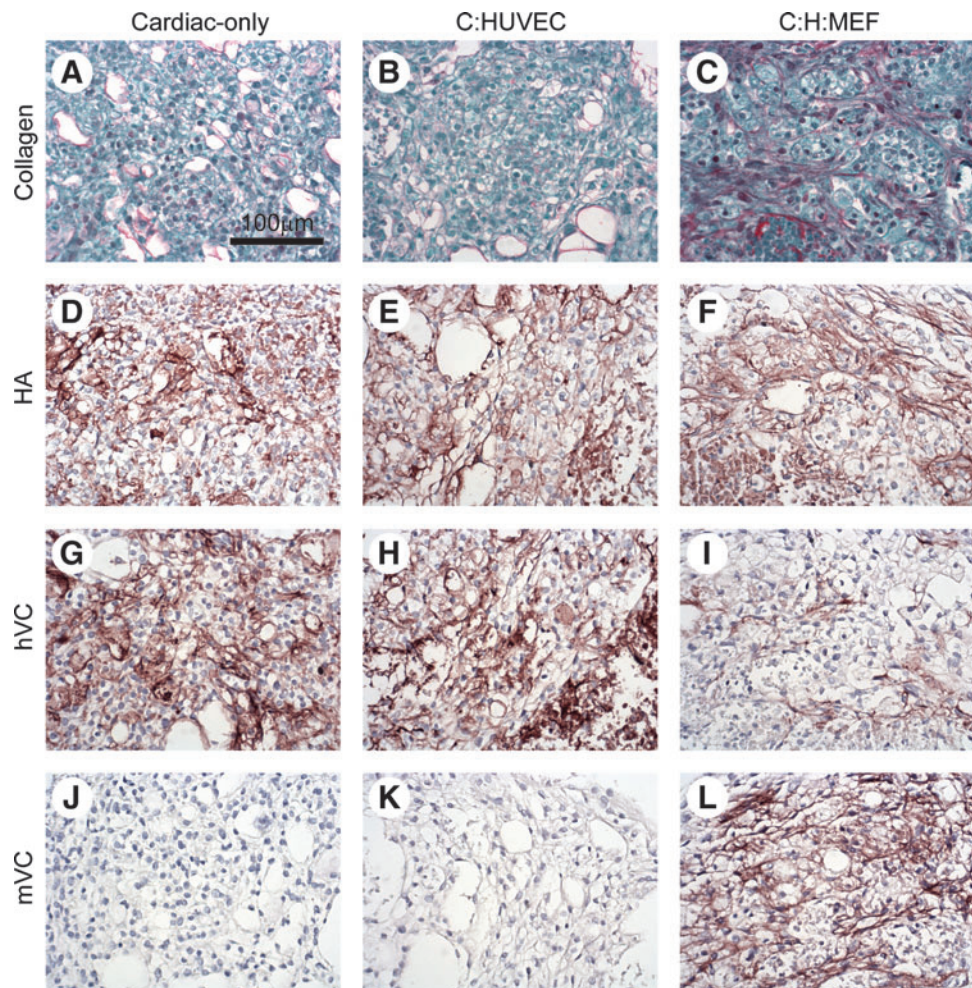


FIG. 2. Extracellular matrix molecules are produced by stromal cells. Patch sections were stained with picosirius red to mark collagen and counterstained with fast green (A–C). Increased production of collagen was observed with addition of MEFs (C) as previously reported.¹¹ Biotinylated hyaluronan (HA) binding protein (brown) demonstrated consistent production of HA in patches with all cell compositions (D–F). Antibodies against human versican (hVC, antibody 2B1) or mouse versican (mVC, antibody AB1033; brown) showed high levels of VC in all patch types (G–L). However, upon addition of MEFs, primarily mouse VC was expressed (L). Scale bar applies to all panels.



different antibodies to versican gave different patterns of staining among the different cell combinations. 2B1, known to stain human versican,³² gave strong staining in cardiac-only and cardiac:HUVEC patches (Fig. 2G, H) but weak staining in cardiac:HUVEC:MEF patches (Fig. 2I). On the other hand, AB1033, which was made against mouse versican and stains mouse tissues,³³ did not stain cardiac-only and cardiac:HUVEC patches (Fig. 2J, K) but did strongly stain cardiac:HUVEC:MEF patches (Fig. 2L). Although species specificities of the two different antibodies have not been thoroughly examined, these results suggest that human cardiomyocytes produce versican in cardiac-only patches, but that versican production is assumed by the mouse stromal cells in tri-cell patches containing MEFs. However, more information regarding the immunoreactivity of the two different antibodies on versican fragments in the two species needs to be ascertained before definitive conclusions can be drawn. Further, although it appears that hESC-derived cardiomyocytes produce sufficient ECM to create a tissue patch and sustain themselves, they alone are unable to support endothelial cell network formation as observed with cardio:HUVEC patches (Fig. 1B). These data indicate that the stromal cells in tri-cell cardiac patches contribute significantly to formation of a rich ECM capable of supporting *in vitro* vascularization.

Clonal lines of hMSCs vary in their ability to support endothelial cell networks in vitro

Knowing that stromal cell populations such as MEFs, NHDFs, and hMSCs are heterogeneous, we hypothesized that clonal sub-populations of stromal cells have varying abilities to support endothelial cell networks in cardiac tissue patches. To test this hypothesis, we formed patches with two clonal lines of hMSCs (HS-5 and HS-27a) that were previously shown to have different gene expression patterns and abilities to support *in vitro* hematopoiesis.^{25,26} Tri-cell cardiac patches at 8 days showed that HS-5 hMSCs do not support the survival or organization of endothelial cells, but that HS-27a hMSCs robustly support endothelial cell networks (Supplementary Fig. S1; Supplementary Data are available online at www.liebertonline.com/tea). To increase the throughput of experiments, we explored this further using bi-cell tissue patches created with HUVECs and stromal cells (without hESC-derived cardiomyocytes). Examining these patches over 8 days of culture shows that, at day 3 (the earliest time examined), both HS-5 and HS-27a hMSCs do support endothelial cell organization into networks, although more efficiently in patches with HS-27a hMSCs (158 ± 117 vs. 377 ± 3 vessel-like structures mm^{-2} ; Fig. 3A top). However, vessel-like structures decreased from day 3 to 8 in both bi-cell vascular patch types, resulting in almost total loss of vessel-like structures in H:HS-5 patches ($14 \pm 1 \text{ mm}^{-2}$) and significant preservation in H:HS-27a patches ($134 \pm 8 \text{ mm}^{-2}$; Fig. 3A, B). This loss of endothelial cell networks during *in vitro* culture indicates that stabilization of vascular networks is one of the principal functions of stromal cells in our cardiac tissue patches.

To test if soluble factors produced by stromal cells are responsible for the difference in pro-vascular phenotype, we generated the conditioned medium from the two stromal lines and performed “media switch” experiments. Growth of bi-cell H:HS-5 patches in the medium conditioned on HS-27a hMSCs did not enhance endothelial networks, and, conversely, HS-5-

conditioned medium did not inhibit networks in H:HS-27a patches (data not shown). This suggests that a soluble inhibitor or stimulator of endothelial cell organization and stabilization is not secreted by the hMSC clones into the medium in large enough quantities to affect vessel formation, and that either direct contact or proximity of MSCs and endothelial cells was required. Using GFP-transduced hMSC clones, we observed the location of hMSCs in relation to hCD31-labeled HUVECs in tri-cell patches (Fig. 3C). While neither the HS-5 nor HS-27a hMSCs take on the morphology of a pericyte or smooth muscle cell around the hCD31-positive structures, the GFP-positive HS-27a hMSCs are interspersed within and found closely apposed to the hCD31-positive vessel structures, whereas endothelial cells are isolated from the HS-5 hMSCs in C:H:HS-5 patches. This suggests that cell-cell interactions may be important for prevascularization of patches. Use of these two hMSC clones provides a platform for further investigating endothelial cell network formation in a tissue-engineered scaffold-free construct.

Versican expression in engineered tissue patches mimics expression in hMSC clonal lines

Array analysis of HS-5 and HS-27a hMSC clones identified versican as an ECM protein whose expression was 19.6-fold higher in the pro-vascular HS-27a versus HS-5 hMSCs.²⁵ Examination of versican protein and mRNA expression levels in bi-cell vascular patches through 8 days of culture shows that versican is consistently higher in H:HS-27a patches (Fig. 4). The HS-5 patches showed little versican protein by immunostaining at any time, whereas HS-27a patches had increasing versican staining (Fig. 4A). Quantitative reverse transcriptase-polymerase chain reaction showed that HUVEC monocultures (i.e., input cells for patches) make very little versican. In contrast, monocultures of HS-27a hMSCs synthesized abundant levels of versican transcripts, with levels 6–23 times greater than HS-5 hMSC monocultures for all versican isoforms. Concordantly, in bi-cell patches, mRNA expression levels were substantially higher in H:HS-27a patches at all time points versus H:HS-5 patches (Fig. 4B). This is most prominent in the abundant, long versican isoforms V0 and V1, but is also true for the shorter versican splice variants V2 and V3 (except V3 on day 5) where expression levels were much lower. These data suggest that ECM deposition in engineered tissue patches reflects the genotype/phenotype of the stromal cells themselves.

Formation of functional vessels in vivo is predicted by endothelial cell network formation in vitro

We hypothesized that differences in vascular network formation *in vitro* would reflect differences in vessel formation after *in vivo* transplantation on the heart. To test this, we implanted tri-cell human cardiac patches (C:H:hMSC, C:H:HS-5 or C:H:HS-27a at day 6 of culture) on the epicardial surface of uninjured athymic rat hearts. All patches were found at 1 week. Patch thickness through the center of the patch was $770 \pm 84 \mu\text{m}$ for C:H:hMSC patches (or about 30% of the total thickness of the heart wall) and not significantly different for C:H:HS-5 and C:H:HS-27a patches. At 1 week, hCD31-positive microvessels with lumens were numerous in C:H:HS-27a implants and nonexistent in C:H:HS-5 implants (Fig. 5A–D). In both cases, patch implants were in contact with the

FIG. 3. Endothelial cell network formation varies with clonal hMSC lines HS-5 and HS-27a in bi-cell patches. An antibody against rabbit CD31 marked endothelial cells (brown) throughout 8 days of *in vitro* culture for two-cell patches with HUVECs and either HS-5 or HS-27a hMSCs (**A**). Endothelial cell networks were more abundant in H:HS-27a patches compared to H:HS-5 patches at all time points. Further, the number of vessel-like structures per mm² decreased with time in culture (**B**; * $p < 0.05$ vs. H:HS-5 on same day; # $p < 0.05$ vs. previous time point with same cell composition). Compressed z-stacks taken with confocal microscopy show GFP-positive clonal hMSCs (green), hCD31-positive HUVECs (red), and blue nuclei (**C**). HUVECs and HS-27a hMSCs are closely apposed in day 8 tri-cell patches (bottom) but HUVECs and HS-5 hMSCs are somewhat isolated from each other (top). Scale bars apply to all panels of (**A**) or (**C**).

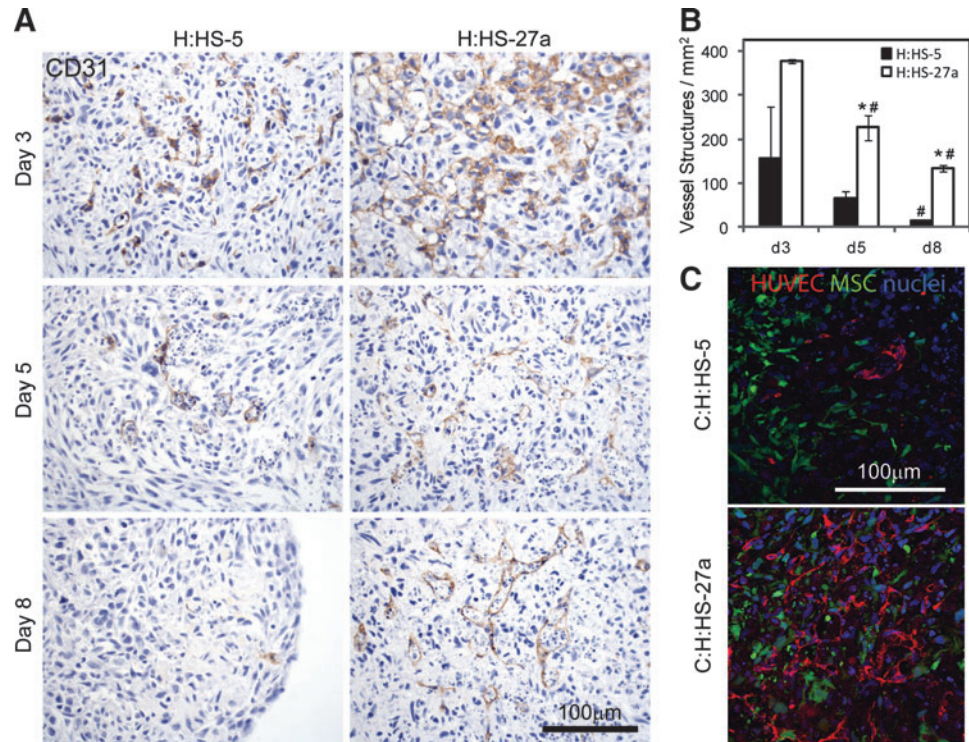
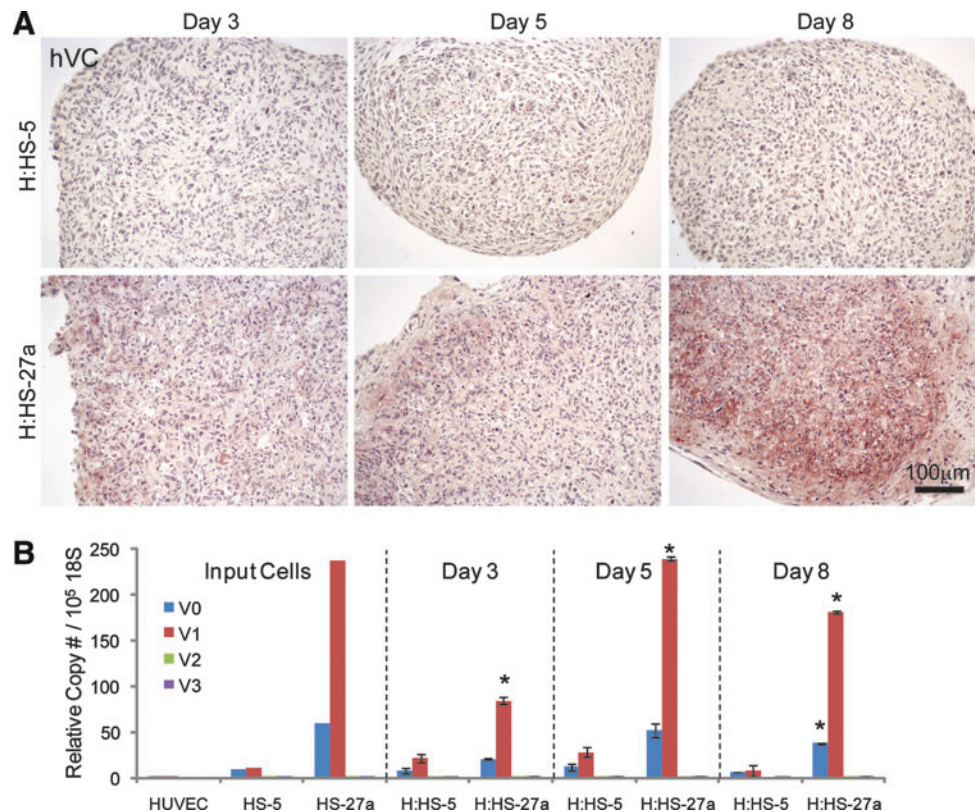


FIG. 4. Versican mRNA and protein are expressed in bi-cell vascular patches but to a greater extent in patches with HS-27a hMSCs. An antibody against human versican (hVC) demonstrated accumulation of versican in H:HS-27a patches through 8 days of culture, whereas versican protein was mostly absent in H:HS-5 patches (**A**). Quantitative reverse transcriptase-polymerase chain reaction for the four splice variants of versican (V0, V1, V2, and V3) shows that V0 and V1 expression predominate (**B**; * $p < 0.05$ vs. H:HS-5 isoform on same day). Both hMSC clones show versican expression at day 0 (input cells), but versican mRNA is consistently more abundant in patches containing HS-27a hMSCs throughout 8 days of culture. Scale bar applies to all panels of **A**.



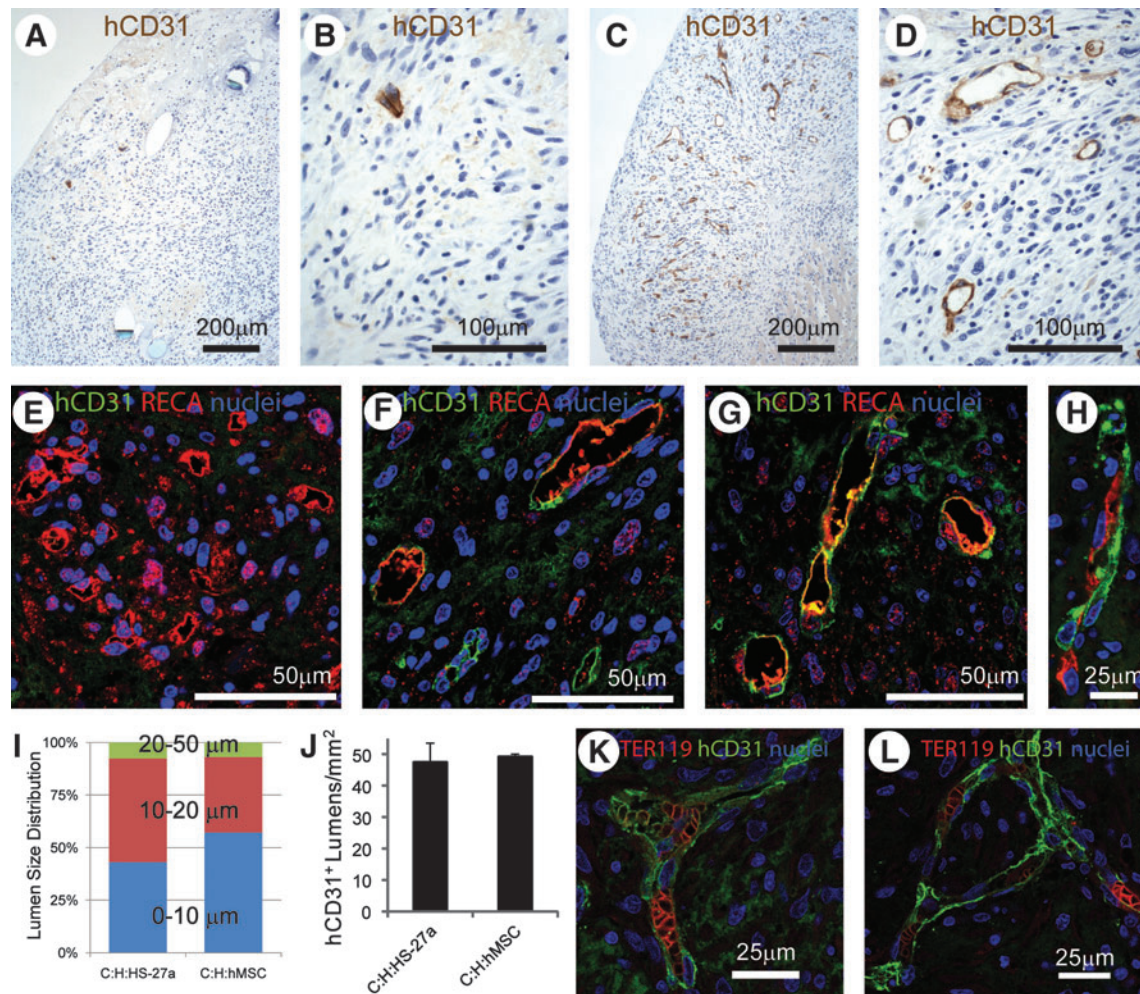


FIG. 5. *In vivo* implantation of tri-cell patches on an uninjured rat heart shows human vessel formation is predicted by the presence of endothelial cell networks *in vitro*. Tri-cell patches with either HS-5 or HS-27a hMSCs were sutured on the epicardial surface of an uninjured athymic rat heart. An antibody to hCD31 (brown) demonstrates few human endothelial cells and no lumen structures in C:H:HS-5 patches (A, B). In contrast, hCD31-positive endothelial cells and lumens are numerous in C:H:HS-27a patches (C, D). Double staining with RECA (red) and hCD31 (green) antibodies demonstrates primarily rat lumens in C:H:HS-5 patches (E) and rat, human, or chimeric lumens in C:H:HS-27a patches (F, G) and in C:H:primary hMSC patches (H). The distribution of lumen diameters was comparable between C:H:HS-27a and C:H:primary hMSC patches, with all lumens being $<50 \mu\text{m}$ (I). The number of hCD31-positive lumens was not different between C:H:HS-27a and C:H:primary hMSC patches (J). The presence of red blood cells marked by TER-119 (red) in hCD31-positive lumens (green) in C:H:HS-27a patches (K) and C:H:primary hMSC patches (L) demonstrates perfusion from the host. RECA, rat endothelial cell antigen.

host heart tissue and no scarring was visible at the interface. A double stain for rat endothelium (RECA antibody) and human endothelium (hCD31 antibody) clearly showed that rat vessels were present in the C:H:HS-5 patches (Fig. 5E) and that rat, human, and rat-human chimeric vessels were present in the C:H:HS-27a patches (Fig. 5F, G). These chimeric vessels with rat and human endothelium were also present in tri-cell patches containing primary hMSCs (Fig. 5H). The average diameter of human vessels was $12.3 \pm 5.8 \mu\text{m}$ (mean \pm SD; $n = 132$) in C:H:HS-27a patch implants and $10.9 \pm 6.0 \mu\text{m}$ ($n = 259$, $p < 0.05$) in C:H:primary hMSC patch implants, with over 90% of the lumens being $<20 \mu\text{m}$ in diameter (Fig. 5I). The human vessel density was 48 ± 6 hCD31-positive lumens per mm^2 in the HS-27a patches and 49 ± 1 lumens per mm^2 in the primary hMSC patches (not significant; Fig. 5J). Finally,

red blood cells (originating from the rat host) stained by TER-119 antibody were present in human vessels from both C:H:HS-27a and C:H:primary hMSC patch implants (Fig. 5K, L). Thus, implantation of human cardiac tissue patches containing endothelial cell networks facilitates rapid (within 1 week) formation of human vessels that anastomose with the host circulation. Further, the ability of stromal cells to support vessel-like networks *in vitro* predicts their ability to support human vessel formation *in vivo*.

Discussion

This study describes the role played by stromal cells in producing extracellular matrix (ECM) and promoting vascularization in scaffold-free engineered human myocardium.

The novel findings include improvement of *in vitro* formation of endothelial cell networks using hMSCs, characterization of the ECM produced in this tissue, development of a platform for investigating how endothelial networks form (with either HS-5 or HS-27a hMSC clonal lines), and demonstration that endothelial cell networks *in vitro* predict *in vivo* vessel formation.

The choice of stromal cell clearly impacts the success in forming vascular networks. This was shown *in vitro* with clonal hMSCs, where HS-27a hMSCs had greater vessel-like structures versus HS-5 hMSCs (Supplementary Fig. S1), including formation of lumens *in vivo* with HS-27a (but not HS-5) hMSCs (Fig. 5). In addition, primary hMSCs increased the number of vessel-like structures *in vitro* more than two-fold compared to MEFs (Fig. 1F). Our optimized constructs contained ~120 luminal structures per mm², which compares favorably to human engineered cardiac tissue made with tri-culture of hESC-derived cardiomyocytes, HUVECs, and MEFs on biodegradable scaffolds by Caspi *et al.*,¹⁹ where only 5 lumens per mm² were reported. When examined *in vivo* in uninjured rat hearts, both our patches (at 1 week, Fig. 5J) and the biodegradable scaffolds (at 2 weeks) showed ~50 hCD31-positive lumens per mm²,¹⁰ suggesting that in a short time both types of engineered tissues provide graft-derived vessels to support implanted cardiomyocytes. Further, both types of engineered tissues also showed host-derived vasculature in the grafts (Fig. 5E–H). Finally, examining the size of these human lumens shows a major difference in these two engineered tissues: Lesman *et al.* report only about 30% of lumens within human vessels were <100 μm in diameter,¹⁰ whereas all human lumens were <50 μm in our cardiac patches (Fig. 5I). The physiological consequence of this size difference is not certain. While tissue clearly cannot be perfused without a capillary network, for robust flow the tissue grafts require an arterial input. Analysis of the origins of graft flow will require further study. In any case, the current data indicate that the quality of microvessels formed *in vivo* can be controlled by carefully selecting stromal cell type *in vitro*.

Stromal cells have the potential to differentiate into mural cells (vascular smooth muscle cells or pericytes) and therefore may provide stabilization of engineered vessels.²⁰ We observed that GFP-positive HS-27a hMSCs were present throughout the web of hCD31-positive endothelial cells *in vitro* (Fig. 3C). While the hMSCs were closely apposed to the endothelial cells, they did not assume classic mural cell morphology. Tracking these stromal cells *in vivo* is a high priority, as Lesman *et al.* reported mouse-derived alpha-smooth muscle actin-positive cells surrounding human microvessels, suggesting differentiation of MEFs into mural cells.¹⁰ Additionally, a minimally immunogenic cell source would aid in translation of engineered cardiac tissue to the clinic. We found that in all implants, regardless of cell composition, there was an influx of CD68-positive macrophages at 1 week (Supplementary Fig. S2). Further study will be required to determine how this macrophage infiltration impacts remodeling of the graft and its ECM, whether these cells promote angiogenesis, and so on.³⁴ The hMSCs derived from human bone marrow used in our current study are clinically available and could be an autologous cell source, which argues for continued use of this cell type in further studies. A renewable source of cardiac stromal cells arises

from human pluripotent stem cell-derived cardiovascular progenitor cells, which are capable of differentiating into vascular smooth muscle cells in addition to cardiomyocytes and endothelial cells.³⁵ These pluripotent stem cells could be hESCs that are HLA-matched for host compatibility³⁶ or human-induced pluripotent stem cells from autologous somatic cells.

Stromal cells in any tissue produce ECM, and this is no different in engineered tissues. We demonstrated that MEFs produce fibrillar collagen (Fig. 2C), which likely increases the tissue's stiffness.¹¹ The use of MEFs with human cardiomyocytes and endothelial cells allowed us to explore which cell population produced the proteoglycan versican (Fig. 2), which may be essential for endothelial cell network formation and stabilization (Figs. 3 and 4). In the absence of stromal cells, cardiac-only and cardiac:HUVEC patches produced human versican (presumably from the cardiomyocyte preparations, since monocultures of HUVECs expressed very little versican [Fig. 4B]). When MEFs were added, production of human versican dropped markedly, and mouse versican was abundant. This suggests a negative feedback loop, where human cardiomyocytes sense versican in the ECM and down-regulate its production when other cells are producing it. It will be interesting to determine if reducing matrix production enhances cardiac differentiation, for example, by augmenting contractile activity, as is observed with other cell types. Smooth muscle cells, for example, are known to have both contractile and synthetic phenotypes, and reduction in ECM synthesis is accompanied by increasing responses to contractile agonists.³⁷

Differences in the ability of clonal hMSC lines to support endothelial networks *in vitro* translated into large differences in formation of human vessels after *in vivo* transplantation. These observations validate the use of our patch tissue engineering system as a means to understand *in vivo* vascularization. The clonal hMSC lines should prove useful in identifying molecules that either promote or inhibit vascular network formation and stabilization. It is well known that cell-matrix interactions influence endothelial cell behavior,²⁹ and here we found that high versican production correlates with the ability of stromal cells to support vascular networks. In fact, a role for versican in stromal cell recruitment and the promotion of angiogenesis in tumorigenesis has recently been demonstrated.³⁸ We hypothesize that versican is an important provisional matrix molecule that promotes formation of stable vascular networks. Further studies in our lab will test this hypothesis in our engineered cardiac tissue patches.

In summary, the rapid creation of vessels *in vivo* is essential to establishing perfusion of cardiac tissue grafts. We previously showed¹¹ that including a preformed vascular network with human endothelium and stromal cells markedly enhanced cardiac patch engraftment. The current study indicates that further gains in vascularization are likely possible through a judicious selection of stromal cell type. These improved vascular networks hasten the establishment of perfusion in cardiac tissue patches, potentially enhancing engraftment and thereby regenerating functional myocardium.

Acknowledgments

We thank Sarah Dupras for surgical expertise and Beverly Torok-Storb for the gift of hMSC clones. This work was

supported by National Institutes of Health Grants R01 HL084642 and P01 HL094374 (to C.E.M.), R24 HL64387 (to C.E.M and T.N.W.), R01 HL18645 (to T.N.W.), by the Experimental Pathology of Cardiovascular Disease Training Grant T32 HL007312 (to K.L.K.), and the UW's Mouse Metabolic Phenotyping Center U24 DK076126.

Disclosure Statement

No competing financial interests exist.

References

- Laflamme, M.A., Chen, K.Y., Naumova, A.V., Muskheli, V., Fugate, J.A., Dupras, S.K., *et al.* Cardiomyocytes derived from human embryonic stem cells in pro-survival factors enhance function of infarcted rat hearts. *Nat Biotechnol* **25**, 1015, 2007.
- Caspi, O., Huber, I., Kehat, I., Habib, M., Arbel, G., Gepstein, A., *et al.* Transplantation of human embryonic stem cell-derived cardiomyocytes improves myocardial performance in infarcted rat hearts. *J Am Coll Cardiol* **50**, 1884, 2007.
- van Laake, L.W., Passier, R., Monshouwer-Kloots, J., Verkleij, A.J., Lips, D.J., Freund, C., *et al.* Human embryonic stem cell-derived cardiomyocytes survive and mature in the mouse heart and transiently improve function after myocardial infarction. *Stem Cell Res* **1**, 9, 2007.
- Zimmermann, W.H., Schneiderbanger, K., Schubert, P., Didie, M., Munzel, F., Heubach, J.F., *et al.* Tissue engineering of a differentiated cardiac muscle construct. *Circ Res* **90**, 223, 2002.
- Carrier, R.L., Papadaki, M., Rupnick, M., Schoen, F.J., Bursac, N., Langer, R., *et al.* Cardiac tissue engineering: cell seeding, cultivation parameters, and tissue construct characterization. *Biotechnol Bioeng* **64**, 580, 1999.
- Radisic, M., Park, H., Shing, H., Consi, T., Schoen, F.J., Langer, R., *et al.* Functional assembly of engineered myocardium by electrical stimulation of cardiac myocytes cultured on scaffolds. *Proc Natl Acad Sci USA* **101**, 18129, 2004.
- Stevens, K.R., Pabon, L., Muskheli, V., and Murry, C.E. Scaffold-free human cardiac tissue patch created from embryonic stem cells. *Tissue Eng Part A* **15**, 1211, 2009.
- Shimizu, T., Yamato, M., Isoi, Y., Akutsu, T., Setomaru, T., Abe, K., *et al.* Fabrication of pulsatile cardiac tissue grafts using a novel 3-dimensional cell sheet manipulation technique and temperature-responsive cell culture surfaces. *Circ Res* **90**, e40, 2002.
- Sekine, H., Shimizu, T., Hobo, K., Sekiya, S., Yang, J., Yamato, M., *et al.* Endothelial cell coculture within tissue-engineered cardiomyocyte sheets enhances neovascularization and improves cardiac function of ischemic hearts. *Circulation* **118**, S145, 2008.
- Lesman, A., Habib, M., Caspi, O., Gepstein, A., Arbel, G., Levenberg, S., *et al.* Transplantation of a tissue-engineered human vascularized cardiac muscle. *Tissue Eng Part A* **16**, 115, 2010.
- Stevens, K.R., Kreutziger, K.L., Dupras, S.K., Korte, F.S., Regnier, M., Muskheli, V., *et al.* Physiological function and transplantation of scaffold-free and vascularized human cardiac muscle tissue. *Proc Natl Acad Sci USA* **106**, 16568, 2009.
- Iyer, R.K., Chiu, L.L., and Radisic, M. Microfabricated poly(ethylene glycol) templates enable rapid screening of triculture conditions for cardiac tissue engineering. *J Biomed Mater Res A* **89**, 616, 2009.
- Rivron, N.C., Liu, J.J., Rouwkema, J., de Boer, J., and van Blitterswijk, C.A. Engineering vascularised tissues *in vitro*. *Eur Cell Mater* **15**, 27, 2008.
- Levenberg, S., Rouwkema, J., Macdonald, M., Garfein, E.S., Kohane, D.S., Darland, D.C., *et al.* Engineering vascularized skeletal muscle tissue. *Nat Biotechnol* **23**, 879, 2005.
- Boland, T., Xu, T., Damon, B., and Cui, X. Application of inkjet printing to tissue engineering. *Biotechnol J* **1**, 910, 2006.
- Kobayashi, A., Miyake, H., Hattori, H., Kuwana, R., Hiruma, Y., Nakahama, K., *et al.* *In vitro* formation of capillary networks using optical lithographic techniques. *Biochem Biophys Res Commun* **358**, 692, 2007.
- Norotte, C., Marga, F.S., Niklason, L.E., and Forgacs, G. Scaffold-free vascular tissue engineering using bioprinting. *Biomaterials* **30**, 5910, 2009.
- Dvir, T., Kedem, A., Ruvinov, E., Levy, O., Freeman, I., Landa, N., *et al.* Prevascularization of cardiac patch on the omentum improves its therapeutic outcome. *Proc Natl Acad Sci USA* **106**, 14990, 2009.
- Caspi, O., Lesman, A., Basevitch, Y., Gepstein, A., Arbel, G., Habib, I.H., *et al.* Tissue engineering of vascularized cardiac muscle from human embryonic stem cells. *Circ Res* **100**, 263, 2007.
- Bergers, G., and Song, S. The role of pericytes in blood-vessel formation and maintenance. *Neuro Oncol* **7**, 452, 2005.
- Arroyo, A.G., and Iruela-Arispe, M.L. Extracellular matrix, inflammation, and the angiogenic response. *Cardiovasc Res* **86**, 226, 2010.
- Li, J., Zhang, Y.P., and Kirsner, R.S. Angiogenesis in wound repair: angiogenic growth factors and the extracellular matrix. *Microsc Res Tech* **60**, 107, 2003.
- Califano, J.P., and Reinhart-King, C.A. Exogenous and endogenous force regulation of endothelial cell behavior. *J Biomech* **43**, 79, 2010.
- Germain, S., Monnot, C., Muller, L., and Eichmann, A. Hypoxia-driven angiogenesis: role of tip cells and extracellular matrix scaffolding. *Curr Opin Hematol* **17**, 245, 2010.
- Graf, L., Iwata, M., and Torok-Storb, B. Gene expression profiling of the functionally distinct human bone marrow stromal cell lines HS-5 and HS-27a. *Blood* **100**, 1509, 2002.
- Roeklein, B.A., and Torok-Storb, B. Functionally distinct human marrow stromal cell lines immortalized by transduction with the human papilloma virus E6/E7 genes. *Blood* **85**, 997, 1995.
- Shukla, S., Nair, R., Rolle, M.W., Braun, K.R., Chan, C.K., Johnson, P.Y., *et al.* Synthesis and organization of hyaluronan and versican by embryonic stem cells undergoing embryoid body differentiation. *J Histochem Cytochem* **58**, 345, 2010.
- Shih, S.C., and Smith, L.E. Quantitative multi-gene transcriptional profiling using real-time PCR with a master template. *Exp Mol Pathol* **79**, 14, 2005.
- Genasetti, A., Vigetti, D., Viola, M., Karousou, E., Moretto, P., Rizzi, M., *et al.* Hyaluronan and human endothelial cell behavior. *Connect Tissue Res* **49**, 120, 2008.
- Wight, T.N. Versican: a versatile extracellular matrix proteoglycan in cell biology. *Curr Opin Cell Biol* **14**, 617, 2002.
- Kenagy, R.D., Plaas, A.H., and Wight, T.N. Versican degradation and vascular disease. *Trends Cardiovasc Med* **16**, 209, 2006.
- Isogai, Z., Shinomura, T., Yamakawa, N., Takeuchi, J., Tsuji, T., Heinemann, D., *et al.* 2B1 antigen characteristically

- expressed on extracellular matrices of human malignant tumors is a large chondroitin sulfate proteoglycan, PG-M/versican. *Cancer Res* **56**, 3902, 1996.
33. Seidelmann, S.B., Kuo, C., Pleskac, N., Molina, J., Sayers, S., Li, R., *et al.* *Athsq1* is an atherosclerosis modifier locus with dramatic effects on lesion area and prominent accumulation of versican. *Arterioscler Thromb Vasc Biol* **28**, 2180, 2008.
 34. Laskin, D.L., Sunil, V.R., Gardner, C.R., and Laskin, J.D. Macrophages and tissue injury: agents of defense or destruction? *Annu Rev Pharmacol Toxicol* **51**, 267, 2011.
 35. Kattman, S.J., Huber, T.L., and Keller, G.M. Multipotent flk-1+ cardiovascular progenitor cells give rise to the cardiomyocyte, endothelial, and vascular smooth muscle lineages. *Dev Cell* **11**, 723, 2006.
 36. Taylor, C.J., Bolton, E.M., Pocock, S., Sharples, L.D., Pedersen, R.A., and Bradley, J.A. Banking on human embryonic stem cells: estimating the number of donor cell lines needed for HLA matching. *Lancet* **366**, 2019, 2005.
 37. Wang, X., Hu, G., and Zhou, J. Repression of versican expression by microRNA-143. *J Biol Chem* **285**, 23241, 2010.
 38. Koyama, H., Hibi, T., Isogai, Z., Yoneda, M., Fujimori, M., Amano, J., *et al.* Hyperproduction of hyaluronan in neuro-induced mammary tumor accelerates angiogenesis through stromal cell recruitment: possible involvement of versican/PG-M. *Am J Pathol* **170**, 1086, 2007.

Address correspondence to:
Charles E. Murry, M.D., Ph.D.
Center for Cardiovascular Biology
Institute for Stem Cell and Regenerative Medicine
University of Washington
815 Mercer St.
Brotman 453
Box 358050
Seattle, WA 98109
E-mail: murry@uw.edu

Received: September 21, 2010

Accepted: December 23, 2010

Online Publication Date: January 28, 2011